URSI - RCRS 2022, IIT (Indore), India, 1 - 4 December, 2022

Investigation of a Broadband Circularly Polarized Printed Monopole Antenna for RF Energy Harvesting Application

Bikash Ranjan Behera* (1), and Sanjeev Kumar Mishra (2)
(1), (2) Advanced RF and Microwave Lab, Department of Electronics and Telecommunication Engineering, International Institute of Information Technology Bhubaneswar, Odisha, India
bikash.r.behera@ieee.org (1), and sanjeev@iiit-bh.ac.in (2)

Abstract

A superstrate-loaded broadband circularly polarized (CP) printed monopole antenna is evaluated for the RF energy harvesting application. For achieving broadband CP traits, enhanced antenna gain and strong directional pattern with wide 3-dB angular beamwidth, circular-shaped monopole having asymmetrical staircased ground plane loaded with PEC superstrate is considered. It is fabricated on the FR-4 substrate with dimension of $1.25\lambda_o \times 1.66\lambda_o \times 0.02\lambda_o$. The proposed prototype exhibits a measured IBW of 5.62 GHz (1.3-6.92 GHz, 136.8%) with ARBW of 1.55 GHz (4.04-5.59 GHz, 32.22%), antenna gain > 6.5 dBic, directional pattern with improved front-to-back ratio (FBR), antenna efficiency > 85% in its operating bands (sub-6 GHz).

1. Introduction

The recently progress in wireless communication systems have emerged for the evolution of hybrid wireless cellular networks. Such types of hybrid networks forms analog & digital topology, requires large bandwidth responses, high antenna gain, enhanced system capacity, etc. for efficient signal coverage in the small base station. So, CP RF front-ends are in high demand due to its benefits and require the technical attributes: low profile, high gain, and maximum polarization performances, which served as vital resource for surrounding wireless connectivity. Also, in the present times, exponential rise for hybrid wireless communication system offers inherent qualities due to reliable QoS, wide channels, low-latencies, along with RF energy harvesting application targeting sub-6 GHz frequency bands [1-4].

In [5-14], CP has been achieved due to the utilization of metamaterials and metasurfaces [5-12], change in feeding mechanism [13], incorporation of fractal [14] as possible techniques, but attainment of limitations is important [15]. By implementing the metasurfaces just below the printed monopole antenna [16], enhances the CP performances in a significant manner, but attaining broadened ARBW and enhanced CP antenna gain of > 6.5 dBic with polarization diversity will always be a challenge and it still needs to be solved from application perspective. So, PEC superstrate-inspired printed monopole antenna with the broadband CP & strong directional pattern are investigated. Their design analogy, working mechanism, corresponding outcomes, & their interpretation from RF energy harvesting prospective are discussed in the subsequent sections.

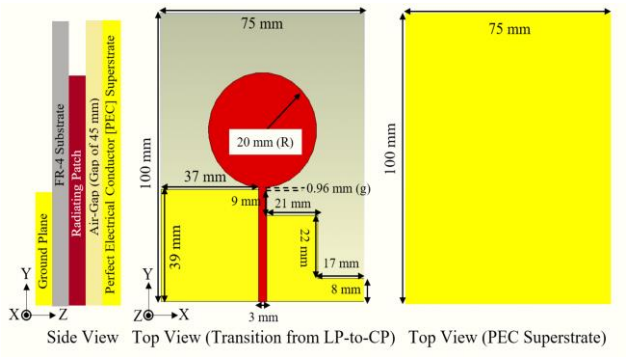

(a)

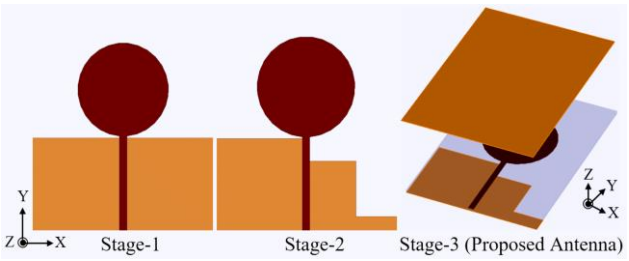

(b)

Figure 1. (a) Schematic configuration and the (b) Design evolution stages of the proposed PEC superstrate antenna.

2. Antenna Design

2.1 Proposed Antenna Configuration

The geometry of proposed antenna is shown in Figure 1 (a), printed on FR-4 substrate with dimension of $1.25\lambda_o \times 1.66\lambda_o \times 0.02\lambda_o$ (λ_o is considered as a guided wavelength at 5 GHz). Its designing process involves 3 stages shown in Figure 1 (b). A detailed insight about them is presented, along with their corresponding outcomes in Figures 2 (a) and (b) respectively.

2.2 Understanding The CP Characteristics

Here, the understanding of CP mechanism is interpreted by utilizing the surface current distribution [approach-I],

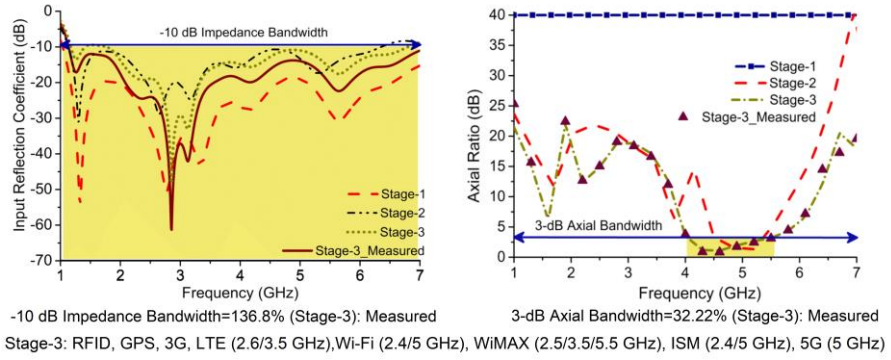

(a)

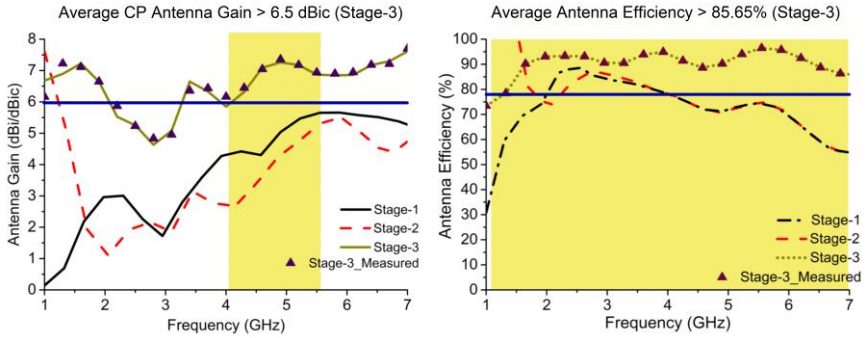

(b)

Figure 2. (a) IBW and ARBW, (B) Antenna gain (LP/CP) and Antenna efficiency from Stage-1 (initial) to Stage-3 (final).

electric field distribution [approach-II], & finally, far-field radiation pattern [approach-II], shown in the Figure 3.

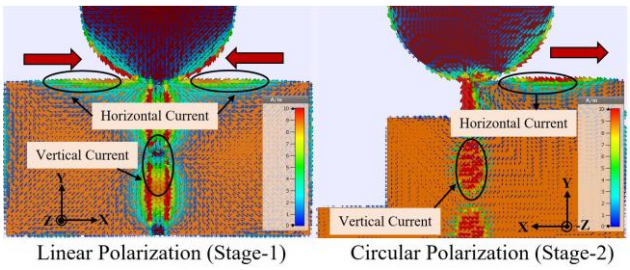

(a)

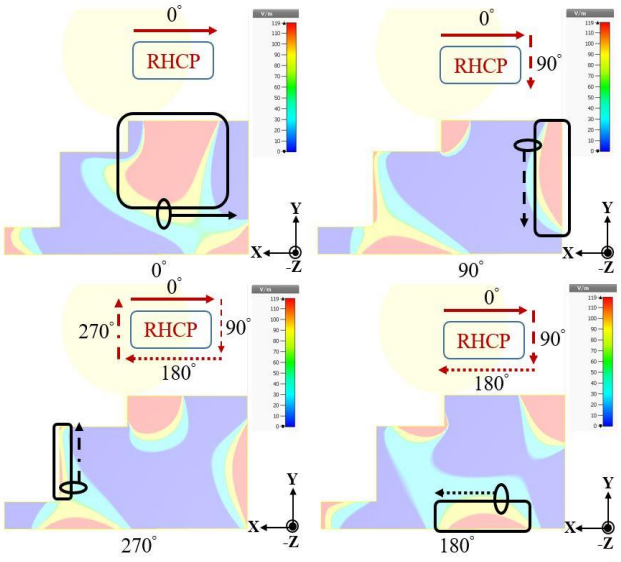

(b)

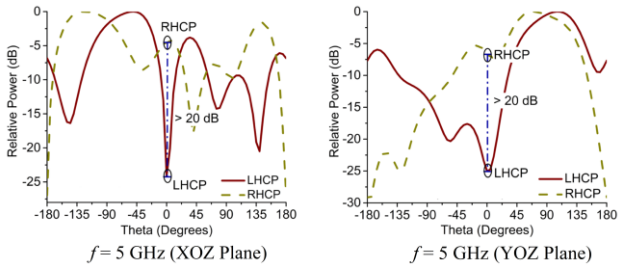

(c)

Figure 3. (a) Analysis of CP mechanism using 3 different approaches at *f*=5 GHz: (a) approach-I, (b) approach-II, & (c) approach-III.

Some of the key observations w.r.t. Figure 3 is given by:

- **Approach-I:** Analysis of surface current distribution, to confirm the existence of CP waves.
- **Approach-II:** Analysis of electric field distribution, to determine the nature of CP waves (RHCP/ LHCP).
- **Approach-III:** Study of relative power related from normalized radiation pattern, to determine the nature of CP (RHCP/LHCP)
- **Final Inference:** The proposed antenna is of RHCP nature, due to its dominancy over the LHCP.

2.3 Incorporation of PEC Superstrate

The incorporation of PEC superstrate of thickness $0.003\lambda_o$ is placed just above CSPMA at height of $0.75\lambda_o$, exhibits broadened impedance bandwidth of 5.54 GHz (1.34-6.88 GHz, 134.8%), 3-dB axial ratio bandwidth of 1.47 GHz

(4.07-5.54 GHz, 30.59%), with average CP antenna gain of 6.56 dBic in their desired operating bands (sub-6 GHz).

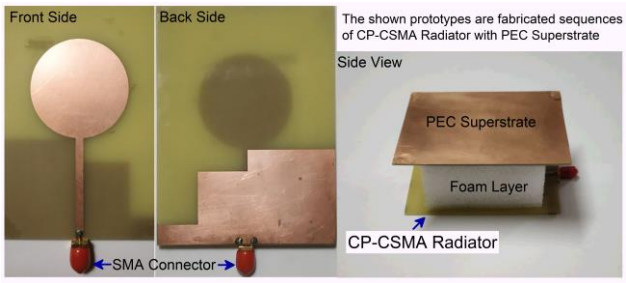

Figure 4. Prototype of proposed PEC superstrate printed monopole antenna.

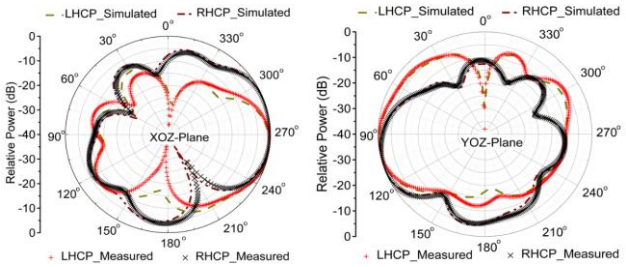

Figure 5. Simulated and measured radiation pattern at 5 GHz of the proposed PEC superstrate antenna.

Table 1(a). Comparison between Stage-2 & Stage-3 (i.e., without and with the presence of PEC superstrate).

Parameters	Stage-2	Stage-3
Geometry	Without PEC Superstrate	With PEC Superstrate
S_{11}	1.1-6.8 GHz	1.34-6.88 GHz
IBW ^{I}	5.7 GHz	5.54 GHz
IBW ^{II}	144.3%	134.8%
Axial Ratio	4.65-5.37 GHz	4.07-5.54 GHz
ARBW ^{I}	720 MHz	1.47 GHz
ARBW ^{II}	14.1%	30.59%
Antenna Gain ^{average}	2.3 dBic	6.56 dBic
HPBW	76.8°	130°
Pattern	Omni-Directional	Directional
Trade-offs [15]	Not Satisfied	Satisfied

Table 1(b). Comparison between simulated and measured outcomes [Stage-3, PEC Superstrate Monopole Antenna].

Parameters	Stage-3	Stage-3
Execution	Simulated	Measured
S_{11}	1.34-6.88 GHz	1.3-6.92 GHz
IBW ^{I}	5.54 GHz	5.62 GHz
IBW ^{II}	134.8%	136.8%
Axial Ratio	4.07-5.54 GHz	4.04-5.59 GHz
ARBW ^{I}	1.47 GHz	1.55 GHz
ARBW ^{II}	30.59%	32.22%
Antenna Gain ^{average}	6.56 dBic	6.61 dBic
HPBW	130°	130°
Pattern	Directional	Directional
Trade-offs [15]	Satisfied	Satisfied

3. Fabrication & its Experimental Validation

To validate the proposed antenna, prototype is fabricated by ETS-PCBMATE prototyping machine, as in Figure 4. S_{11} is measured by using a PNA X-series VNA (N5247A) from Keysight Technologies whereas the ARBW, antenna gain, radiation pattern, & antenna efficiency are measured in the anechoic chamber. Standard high-gain horn antenna from Pasternack (WR-187), 2021 model is used; designed antenna is acting as test antenna for measurement of far-field parameters. Simulated S_{11} < -10 dB is 1.34-6.88 GHz with 134.8% IBW and measured S_{11} < -10 dB is 1.3-6.92 GHz with 136.8% IBW shown in Figure 2(a). The ARBW results shown in Figure 2(a) with the simulated ones from 4.07-5.54 GHz with 30.59% ARBW & the measured ones from 4.09-5.59 GHz with 32.22% ARBW. Figure 2(b), shows the antenna gain & efficiency. Here, the simulated peak and measured peak gain lies in between 5-7.52 dBic, and measured efficiency > 85% in their operating bands. A detailed study is shown in Table 1. The simulated and measured radiation patterns (2D) are shown at *f*=5 GHz in Figure 5 with attained front-to-back ratio of > -21.5 dBic.

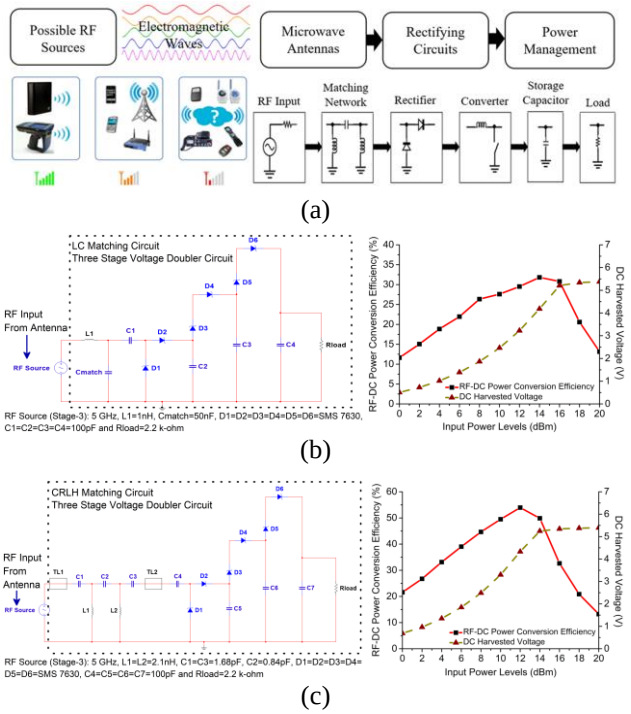

Figure 6. Implementation of the rectifier circuit for η_o and V_{out}: (a) Block Diagram, (b) Circuit-I, and (c) Circuit-II.

4. Analysis Towards RF Energy Harvesting: Design Perspective

Here, the proposed superstrate antenna is integrated with the LC-based Greinacher voltage doubler circuits (GVD), in which the RF-to-DC conversion efficiency (η_o, %) and DC harvested voltage (V_{out}, V) are calculated by using the ADS circuit solver. Complete block diagram of RF energy harvesting mechanism, and their corresponding outcomes are shown in the Figures 6(a)-(c). In the next, considering its execution, large-signal S-parameter circuit simulation

(LSSP) environment is setup in the ADS circuit solver to determine the various outcomes. Thus, η_o is calculated by considering equation-(1), is analyzed for the input power levels (P_{in}) from -10 dBm to +20 dBm at the 5 GHz. On testing in ADS with the load resistance (R_{load}) of 2.2 kΩ, the V_{out} is 3.22 V, figure of merits (FOM) is 94.82 with η_o calculated as the 29.45% at 12 dBm (circuit-I) and V_{out} is 4.33 V, figure of merits (FOM) is ~213 with η_o calculated as 53.26% at 12 dBm (circuit-II) are obtained out. A brief analysis about the interpretation of its outcomes is shown in Table 2.

$$\eta_o = \frac{P_{load}}{P_{incident}} = \frac{V_{out}^2}{P_{in} \times R_{load}} \times 100\% \text{.....(1)}$$

Table 2. Comparison of performance metrics (RF energy harvesting application) of the proposed antenna [Stage-3].

Configuration	P_{in} (5 GHz)	η_o (%)	V_{out} (V)
Circuit-I	12 dBm	29.45%	3.22 V
Circuit-II	12 dBm	53.26%	4.33 V

5. Conclusion

A broadband CP superstrate inspired monopole antenna is presented. It exhibits broadened IBW and ARBW with CP gain > 6.5 dBic, antenna efficiency > 85% in their desired band, which is quite better than these conventional printed monopole antennas as well as to the reported ones [5-14] inducted in the literature review. Insights about attainment of CP is backed by 3 different approaches are reported. In the later part, impact of matching circuits, finding figure-of-merits (FOM), RF-DC conversion, and DC harvested voltage is evaluated, by just looking from the application perspective.

6. References

1. AT Abed, "A novel coplanar antenna butterfly structure for portable communication devices," *IEEE Antennas and Propagation Magazine*, Vol. 62, No. 3, pp. 83-89, 2020.

2. BY Toh, *et al*., "Understanding and measuring circular polarization," *IEEE Transactions on Education*, Vol. 46, No. 3, pp. 313-318, 2003.

3. MJ Maybell, "A polarization basics diagram [Historical corner]," *IEEE Antennas and Propagation Magazine*, Vo- l. 61, No. 1, pp. 130-135, 2019.

4. D Surender, *et al*., "Rectenna design and development strategies for wireless applications," *IEEE Antennas and Propagation Magazine*, pp. 2-15, 2021 (Early Access).

5. T Nakamura, *et al*., "Broadband design of circularly polarized microstrip patch antenna using artificial ground structure with rectangular unit cells," *IEEE Transactions on Antennas and Propagation*, Vol. 59, No. 6, pp. 2103-2110, 2011.

6. W Yang, *et al*., "Novel polarization rotation technique based on artificial magnetic conductor and its application in low-profile circular polarization antenna," *IEEE Trans--action on Antennas Propagation*, Vol. 62, No. 12, pp. 6206-6216, 2014.

7. Z Wu, *et al*., "Metasurface superstrate antenna with wi--deband circular polarization for satellite communication application," *IEEE Antennas and Wireless Propagation Letters*, Vol. 15, pp. 374-377, 2016.

8. T Yue, *et al*., "Compact, wideband antennas enabled by interdigitated capacitor-loaded metasurfaces," *IEEE Tran--sactions on Antennas and Propagation*," Vol. 64, No. 5, pp. 1595-1606, 2016.

9. J Chatterjee, *et al*., "Broadband circularly polarized H-shaped patch antenna using reactive impedance surface," *IEEE Antennas and Wireless Propagation Letters*, Vol. 17, No. 4, pp. 625-628, 2018.

10. Q Chen, H Zhang, H-F Yang, *et al*., "Wideband and low axial ratio circularly polarized antenna using AMC-based structure polarization rotation reflective surface," *International Journal of Microwave and Wireless Techn--ologies*, Vol. 10, No. 9, pp. 1058-1064, 2018.

11. S S Jash, C Goswami, and R Ghatak, "A low profile broadband circularly polarized planar antenna with an em--bedded slot realized on a reactive impedance surface," *AEUE-International Journal of Electronics and Commun--ications*, Vol. 108, pp. 62-72, 2019.

12. L Huang, *et al*., "Design of a compact wideband CP metasurface antenna. *International Journal of RF and Mi--crowave Computer-Aided Engineering*, Vol. 30, No. 10, e22332, 2020.

13. R Kumar, S. R. Thummaluru, *et al*., "Improvements in Wi-MAX reception: A new dual-mode wideband circula--arly polarized dielectric resonator antenna," *IEEE Anten--nas and Propagation Magazine*, Vol. 61, No. 1, pp. 41-49, 2019.

14. A Altaf, Y Yang, *et al*., "Circularly polarized spidron fractal dielectric resonator antenna," *IEEE Antennas and Wireless Propagation Letters*, Vol. 14, pp. 1806-1809, 2015.

15. B R Behera, P R Meher, and S K Mishra, Microwave antennas-An intrinsic part of RF energy harvesting syste--ms: A contingent study about its design method ologies and state-of-art technologies in current scenario," *Interna--tional Journal of RF and Microwave Computer-Aided Engineering*, Vol. 30, No. 5, pp. 1-27, e22148, 2020.

16. M Ameen and R. Chaudhary, "Metamaterial circularly polarized antennas: Integrating an epsilon negative trans--mission line and single split ring-type resonator. *IEEE Antennas and Propagation Magazine*, Vol. 63, No. 4, pp. 60-77, 2021.